

Search for the proton decay $p \rightarrow K^+\bar{\nu}$ in the large liquid scintillator low energy neutrino astronomy detector LENA

T. Marrodán Undagoitia,^{1,*} F. von Feilitzsch,¹ M. Göger-Neff,¹ C. Grieb,² K. A. Hochmuth,¹ L. Oberauer,¹ W. Potzel,¹ and M. Wurm¹

¹*Physik-Department E15, Technische Universität München,
James-Frank-Str., 85748 Garching, Germany*

²*Virginia Polytechnic Institute and State University,
Physics Department, Robeson Hall, Blacksburg,
VA 24061-0435, USA*

The LENA (Low Energy Neutrino Astronomy) detector is proposed to be a large-volume liquid-scintillator device which will be highly suitable for the investigation of a variety of topics in astrophysics, geophysics and particle physics. In this paper, the potential of such a detector concerning the search for proton decay in the SUSY favored decay channel $p \rightarrow K^+\bar{\nu}$ is investigated. Based on Geant4, Monte Carlo simulations of the proton decay in the LENA detector as well as of the background radiation in the detection energy windows have been developed. From these simulations an efficiency of 65% for the detection of a possible proton decay has been determined. Within ten years of measuring time a lower limit for the proton lifetime, concerning the decay channel investigated, of $\tau > 4 \cdot 10^{34}$ y could be reached.

PACS numbers: 13.30-a, 14.20.Dh, 29.40.Mc, 02.70.Uu

I. DETECTOR DESCRIPTION

The LENA (Low Energy Neutrino Astronomy) detector is planned [1] to have a cylindrical shape with about 100 m length and 30 m diameter. An inside part of 13 m radius will contain approximately 50 kt of liquid scintillator while the outside part will be filled with water to act as a muon veto. A fiducial volume for proton decay will be defined having a radius of 12 m. Covering about 30% of the surface, 12000 photomultipliers of 50 cm diameter each will collect the light produced by the scintillator. PXE (phenyl-o-xylylene) is foreseen as scintillator solvent because of its high light yield and its safe handling procedures. The optical properties of a liquid scintillator based on PXE have been investigated in the Counting Test Facility (CTF) for BOREXINO at the Gran Sasso underground laboratory [2]. A yield of 372 ± 8 photoelectrons per MeV (pe/MeV) have been measured in this experiment with an optical coverage of 20%. The attenuation length of ~ 3 m (at 430 nm) was substantially increased to ~ 12 m purging the liquid in a weak acidic alumina column [2]. With these values an expected photoelectron yield of ~ 120 pe/MeV can be estimated for events in the center of the LENA detector. Currently the optical properties of mixtures of PXE and derivatives of mineral oils are under investigation [3].

In addition to astrophysical processes such as supernovae neutrinos, relic supernovae neutrinos and solar

neutrinos also geophysical aspects and research in particle physics, e.g. long baseline experiments and the search for the proton decay will play a major role. Possible locations for this detector, currently under discussion, are an underground mine in the center of Finland (Pyhäsalmi, CUPP: Center of Underground Physics in Pyhäsalmi) or under water, close to the coast at Pylos in Greece. Both sites have a shielding of ~ 4000 meters water equivalent (m.w.e.) and are far away from nuclear power plants, which cause the main contribution to the $\bar{\nu}_e$ background in the measurement of relic supernovae neutrinos.

In this letter the sensitivity of LENA for the search of the proton decay $p \rightarrow K^+\bar{\nu}$ is investigated. The potential of a large liquid scintillator detector for proton decay detection has already been proposed by R. Svoboda [4].

II. THEORETICAL PREDICTIONS

In the Grand Unified Theories (GUTs), the decay of the proton is predicted, leading to a nonconservation of the baryon (B) and lepton (L) numbers. A measurement of such an event could be a probe of the validity of those theories and further evidence for the existence of physics beyond the Standard Model. In the minimal GUT SU(5) [5], the nucleon decays via exchange of gauge bosons with GUT scale masses ($\sim 10^{15}$ GeV). The dominant proton decay mode predicted is $p \rightarrow e^+\pi^0$ with a lifetime of $\tau \sim 10^{31}$ y. The Super-Kamiokande Collaboration has set the current lower limit for this channel to $\tau > 5.4 \cdot 10^{33}$ y at 90% confidence level (C.L.) [6]. This result together with the fact that, in this theory, the three running coupling constants do not meet in a single point

*Corresponding author. Fax: +49 89 289 12680, Telephone Number: +49 89 289 12328.; Electronic address: tmarroda@ph.tum.de

give reasons to look also at other theories.

In Supersymmetric GUTs (SUSY), the nucleon decay is affected by operators of dimension 4, 5 and 6. They involve B- and L-violating processes but conserve B-L. For the proton decay mode $p \rightarrow e^+\pi^0$ a lifetime of $\tau \sim 5 \cdot 10^{35 \pm 1}$ y has been calculated. This rather long lifetime results from the large value of the unification mass, M_G , given by those theories. For the decay channel $p \rightarrow K^+\bar{\nu}$ ($\bar{\nu} = \sum_{\{i=e,\mu,\tau\}} \bar{\nu}_i$) a range for the lifetime $\tau \sim (0.33 - 3) \cdot 10^{34}$ y [7] has been predicted. Also previous studies on SUSY theory have found the same decay channel $p \rightarrow K^+\bar{\nu}$ to be the dominant one with a lifetime range of $\tau \sim (10^{30} - 10^{35}$ y) [8]. The kaon produced in the dominant SUSY proton decay channel is ‘invisible’ in water Cherenkov detectors because its momentum is below the threshold for producing Cherenkov light ($T_{th}(K^+) = 253$ MeV). For this reason, the Super-Kamiokande experiment could only perform an indirect measurement with efficiencies of 4.4% and 6.5% corresponding to two different methods [9]. The lower limit that they reach at 90% C.L. is $\tau > 2.3 \cdot 10^{33}$ y [10].

Supergravity theories provide also predictions for the possible decay channels of the proton. The dominant mode here is $p \rightarrow \pi^+\bar{\nu}$ with a branching ratio of 65.7%. However, again the proton decay mode $p \rightarrow K^+\bar{\nu}$ is predicted with a branching ratio of 33.5% [11].

In a scintillation detector like LENA, the K^+ particles from proton decay events can be observed directly. These signals together with the delayed signals from the decay products provide a very distinct signature for this decay mode.

III. DETECTION MECHANISM

Within the detector volume of LENA, about $1.45 \cdot 10^{34}$ protons, both from C- and H-nuclei, are candidates for the decay. This number has been calculated taking into account the chemical composition of PXE ($C_{16}H_{18}$), its density (0.985 g/cm³) and its molecular weight (210.3 a.m.u.).

In the case of protons from H-nuclei ($0.23 \cdot 10^{34}$ protons in the fiducial volume of LENA), the decay problem is simplified because those protons decay at rest. Therefore, the proton decaying in the channel $p \rightarrow K^+\bar{\nu}$ can be considered as a two-body decay problem where K^+ and $\bar{\nu}$ always receive the same energy. The energy corresponding to the mass of the proton, $m_p = 938.3$ MeV is thereby given to the decay products. Using relativistic kinematics, it can be calculated that the particles receive fixed kinetic energies, the neutrino 339 MeV and the kaon 105 MeV.

In the LENA detector, the kaon will cause a prompt mono-energetic signal while the neutrino escapes without producing any detectable signal. After $\tau(K^+) = 12.8$ ns, the kaon decays via $K^+ \rightarrow \mu^+\nu_\mu$ with a probability of 63.43%. In 90% of the times, the kaon decays at rest [9] and from this kaon decay, a second mono-energetic sig-

nal arises, corresponding to the μ^+ with 152 MeV kinetic energy. Later, after $\tau(\mu^+) = 2.2$ μ s, also the muon will decay: $\mu^+ \rightarrow e^+\nu_e\bar{\nu}_\mu$, the e^+ will produce a third long-delay signal. Since the last decay is a three body decay, the e^+ does not have a fixed energy but a spectrum. With a smaller probability, 21.13%, the kaon decays, alternatively, via $K^+ \rightarrow \pi^+\pi^0$. The π^+ deposits its kinetic energy (108 MeV) in the detector. The π^0 decays almost immediately, within $\tau(\pi^0) = 8.4 \cdot 10^{-8}$ ns, into two gammas with a total energy being equal to the sum of the kinetic energy of the π^0 (111 MeV) and its rest mass ($m_{\pi^0} = 135$ MeV). These gammas can be seen in the detector as electromagnetic showers. Thus again there are two mono-energetic signals, firstly the kaon and secondly the one corresponding to the sum of the kinetic energy of the π^+ and the energy of the gammas. Again, there will be a third long-delayed signal from the succeeding decays ($\pi^+ \rightarrow \mu^+\nu_\mu$ and $\mu^+ \rightarrow e^+\nu_e\bar{\nu}_\mu$). Only these two most likely decay channels of the kaon are considered in the analysis.

For the protons of the C-nuclei ($1.22 \cdot 10^{34}$ protons in the fiducial volume of the LENA detector), one has to consider further nuclear effects on the proton decay. First of all, since the protons are bound to the nucleus their effective mass will be reduced by the binding energy. The proton energy available for distribution between the decay products, will be $M'_p = M_p - E_b$, where M'_p is the modified proton mass, $M_p = 938.3$ MeV is the rest mass of the proton and E_b is the nuclear binding energy. The value of the binding energy E_b can be derived from gaussian probability functions which for C-nuclei [12] are centered at 37 MeV and 16 MeV for protons in s-state and p-states, respectively. Secondly, in case of a proton decay in a nucleus, e.g., carbon, decay kinematics are different from the free proton due to the Fermi motion of the proton. These Fermi momenta have been measured by electron scattering on ¹²C [12]. The maximum momentum is about 250 MeV/c.

To determine the kinetic energy change of the decay particles of the proton, various decay processes have been calculated [13]. First of all, the mass of the proton was modified due to the binding energies for s- and p-states according to the values mentioned above. For both, two extreme cases were considered: the neutrino, after the decay, moving in the direction of the original proton and the neutrino moving in the opposite direction, the kaon, of course, always moving in the opposite direction of the neutrino. The momentum of the proton was chosen to be maximal, corresponding to a Fermi momentum of ~ 250 MeV/c. The limiting values for the range of the kinetic energy of the kaon are: (25.1 – 198.8) MeV for the s-state and (30.0 – 207.2) MeV for the p-state.

IV. SIMULATION

In order to quantitatively estimate the potential of the LENA detector for measuring the proton lifetime, a

Monte Carlo simulation for the decay channel $p \rightarrow K^+\bar{\nu}$ has been performed. For this purpose, the Geant4 simulation toolkit has been used [14]. The event generator was programmed to produce K^+ particles of 105 MeV in the center of the detector volume and with random directions. The simulation was also performed for proton decays which do not take place in the center to investigate the dependence on the event position.

Not only all default Geant4 physics lists were included but also optical processes as scintillation, Cherenkov light production, Rayleigh scattering and light absorption. For the last two processes scattering and absorption lengths of $\lambda_s = 60$ m and $\lambda_a = 12$ m, respectively, were assumed. With these numbers an effective attenuation length of $\lambda = 10$ m results from:

$$\lambda = \frac{\lambda_s \cdot \lambda_a}{\lambda_s + \lambda_a} \quad (1)$$

This is a quite conservative approach compared to the measured value of $\lambda = 12$ m [2] and results in a light yield of ~ 110 pe/MeV for an event in the center of the detector. The dependence of the detection efficiency and the photoelectron yield on scattering and absorption lengths will be discussed later (see Chapter 6, Table II).

To determine the detector efficiency, a total of 20 000 $p \rightarrow K^+\bar{\nu}$ Monte Carlo events were generated. Within this simulation, it was possible to verify that the kaons decay according to the branching ratios for the different channels stated in [15]. The amount of light emitted by a scintillating material is not strictly proportional to the energy deposited by the ionizing particle. In reality, it is a complex function of energy, the type of particle and the specific ionization [16]. To take into account the so called quenching effects, the semi-empirical Birk's formula [17] has been introduced into the code:

$$\frac{dL}{dx} = \frac{A \frac{dE}{dx}}{1 + kB \frac{dE}{dx}} \quad (2)$$

The parameters of this formula are A: absolute scintillation efficiency and kB: parameter relating the density of ionization centers to $\frac{dE}{dx}$. Both are specific values for every scintillator and are obtained from experimental data. For the simulation, $A = 10^4$ photons/MeV and $kB = 1.5 \cdot 10^{-2}$ cm/MeV have been taken from studies performed by the BOREXINO Collaboration [18]. According to equation 2, the program calculates in every step the deposited energy (dE) within the distance (dx) travelled by the particle and derives the light output ($\frac{dL}{dx}$).

Also the photomultipliers have been introduced in the simulation assuming an efficiency of 17 % and a time jitter of $\sigma = 1$ ns originating from the transit time of electrons through the photomultipliers and from the statistical noise. These features are known because this type of photomultiplier has already been used in other experiments [19].

V. BACKGROUND REJECTION

A. Muon Production

The main background source in the energy range of the proton decay are muon neutrinos ν_μ produced by cosmic ray interactions in the atmosphere. Atmospheric ν_μ can interact with the scintillator producing muons in the energy range where the search for the proton decay is performed. The rate of these events in the relevant energy range can be derived from the Super-Kamiokande measurements [9]. From this data we find an event rate of:

$$\Gamma \sim 4.8 \cdot 10^{-2} (\text{MeV}^{-1} \text{kt}^{-1} \text{y}^{-1}) \quad (3)$$

where the LENA energy window as well as the volume have to be introduced in MeV and kt, respectively.

In order to distinguish the real proton decay signals from muon background events, a pulse shape analysis can be applied. From the simulation it is known that the kaon deposits its energy in 1.2 ns. Then, as the kaon decays within a relatively short time ($\tau(K^+) = 12.8$ ns), the signature from such an event will consist of two shortly delayed signals. Examples of a proton decay signal where the separation is clearly visible, where it is almost hidden in the risetime and of a muon background signal can be seen in figure 1. The better the two signals can be separated, the better the background suppression will be. In the cases where the kaon decays at late times ($t > 10$ ns), the two peaks can be easily separated; in all other cases, only a shoulder within the risetime can be seen.

The on-set time of these examples is 60 ns as the events are generated at the center of the detector and the photons need this time to reach the photomultipliers.

1. Time Cut

A first step towards a pulse shape analysis has been taken in order to quantify the signal and background discrimination. Not only 20 000 Monte Carlo proton decay events were generated but also 20 000 muon background events for each kaon decay channel analysed. For these simulations, the particles were generated in the center of the detector and the light produced was followed through the scintillator and the photomultipliers. This results in the number of photoelectrons detected as a function of time. From the resulting signal the maximum number of photoelectrons is taken and the 15 % and the 85 % values of the maximum signal height are calculated. The difference of the two corresponding time values is plotted in figure 2.

As an example, a cut at 7 ns is shown in this figure. Applying such a cut, a background reduction by a factor of $\sim 2 \cdot 10^4$ is achieved. The background plot shown applies only to the channel $p \rightarrow K^+\bar{\nu}$ and $K^+ \rightarrow \mu^+\nu_\mu$.

A similar simulation has been performed for the channel $p \rightarrow K^+ \bar{\nu}$ and $K^+ \rightarrow \pi^+ \pi^0$ resulting in an equivalent result where the same rejection factor is obtained. An efficiency of $\varepsilon_T = 0.65$ results after this time cut because only 35% of the signals are lost.

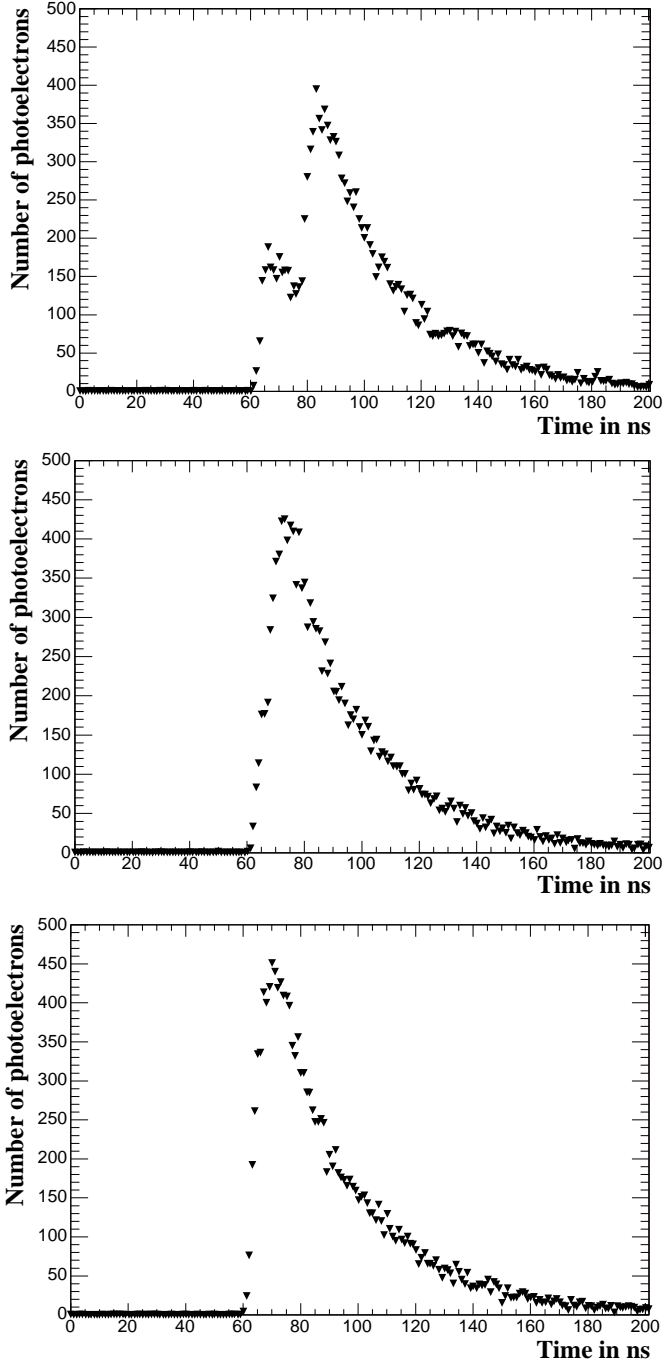


FIG. 1: Proton decay signal where the kaon decays after 18 ns (top) and after 5 ns (middle). The bottom panel shows a ν_μ background signal.

2. Energy Cut

In order to further improve the signal to background separation a cut in the energy spectrum can be applied. Figure 3, shows the distribution of the number of photoelectrons coming from free proton decay events at the center of the detector as seen in the photomultipliers.

Two peaks can clearly be identified, corresponding to the two main decay channels of the kaon. They are related to the energies of 257 and 459 MeV, which is the sum of the energies deposited by the kaon and its decay products (see section Detection Mechanism). For each peak a 300 MeV window has been set resulting in an efficiency of $\varepsilon_E = 0.995$ for this energy cut. The two energy windows overlap resulting in a final window of 500 MeV. The signals outside these energy windows correspond mainly to kaon decay channels not considered in the analysis. There is also a small loss due to inelastic hadronic interactions of the decay particles before they are stopped.

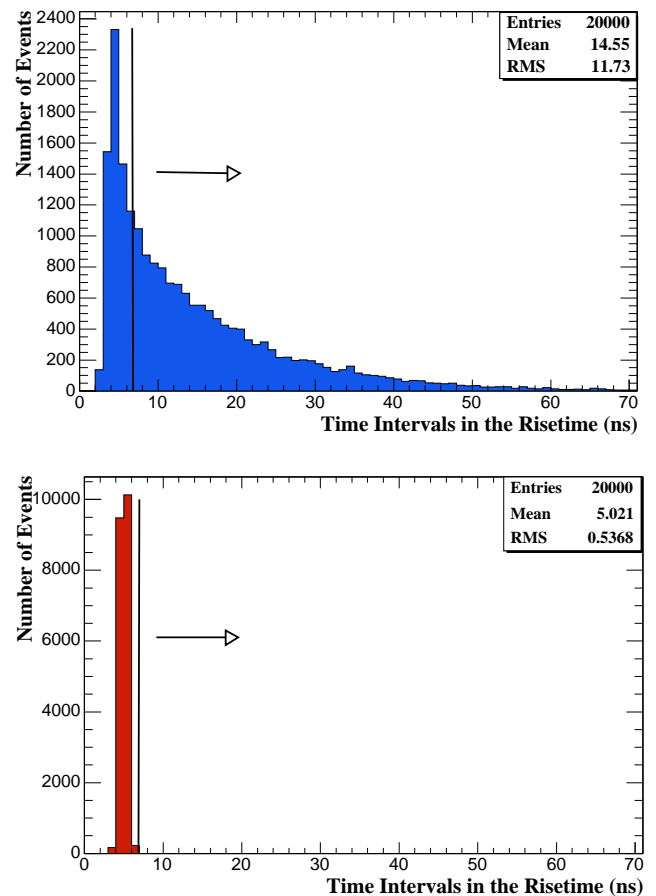


FIG. 2: Distribution of time intervals in the risetimes for proton decay (top) and muon background signals (bottom). A cut at 7 ns yields a reduction factor of $\sim 2 \cdot 10^4$ on background events whereas the efficiency for observing a proton decay $p \rightarrow K^+ \bar{\nu}$ is 65%.

B. Hadron Production

Atmospheric neutrinos can interact with the detector producing also hadrons. The most probable of these reactions is the single pion production [20][21]:

$$\nu_\mu + p \rightarrow \mu^- + \pi^+ + p' \quad (4)$$

In such a reaction, the first signal comes from the sum of the energies deposited by the μ^- and the π^+ . Later, after $\tau_{\pi^+} = 26$ ns, the π^+ decays into μ^+ and one neutrino producing a second short-delay signal. However, the π^+ has such a small mass (139.6 MeV) that its decay muon receives only about 20 MeV kinetic energy. The signal produced by the μ^+ is small. Therefore, those events do not have the same signature as the proton decay signal. Moreover, since the muon signal is so small it is usually hidden behind the above mentioned first signal.

Neutrinos of higher energies can interact producing strange particles, thus also kaon production has to be considered. According to the MINERvA proposal [22], the reactions of this type with notable probability are:

$$\nu_\mu + p \rightarrow \mu^- + K^+ + p \quad (5)$$

$$\nu_\mu + n \rightarrow \mu^- + K^+ + \Lambda^0 \quad (6)$$

$$\nu_\mu + n \rightarrow \mu^- + K^+ + \Lambda^0 + \pi^0 \quad (7)$$

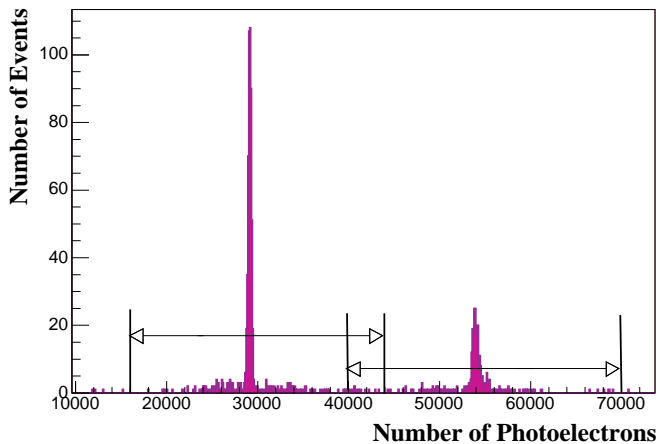


FIG. 3: Distribution of the number of photoelectrons produced in the photomultipliers coming from free proton decay events at the center of the detector. The cuts performed for the two main decay channels of the kaon (at ~ 257 and ~ 459 MeV) are shown. It can be recognized that the energy windows taken overlap resulting in a total window of 55000 photoelectrons $\simeq 500$ MeV.

In equations 6 and 7, to conserve the strangeness number the kaon is produced together with a Λ^0 baryon. This Λ^0 particle decays after $\tau_{\Lambda^0} = 0.26$ ns mainly via two channels $\Lambda^0 \rightarrow p + \pi^-$ (63.9%) or $\Lambda^0 \rightarrow n + \pi^0$ (35.8%). Because of this short lifetime, the p, π^- or n, π^0 cause a prompt signal together with the μ^- , the K^+ and the π^0 in the case of equation 7. The prompt signal in these two reactions is bigger than the signal of the μ^+ from the kaon decay (or π^+ , π^0 if the kaon decays within the second-probable channel). For this reason, the signature of the background signal can be distinguished from proton decay events. Figure 4 shows an example of equation 6. First a big peak can be seen corresponding to the signals of the μ^- , K^+ and Λ^0 . After that, two other peaks appear, one is due to the μ^+ that originates from the decay of the K^+ and the other a μ^- from $\Lambda^0 \rightarrow p + \pi^-$ and $\pi^- \rightarrow \mu^- \bar{\nu}_\mu$.

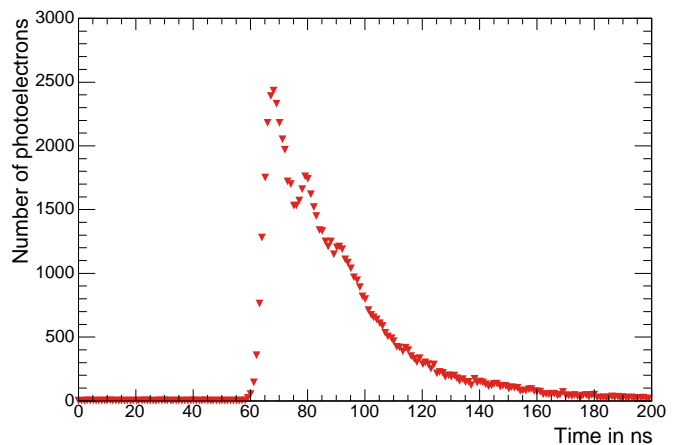


FIG. 4: Background signal for proton decay events. The first peak corresponds to the signals of the μ^- , K^+ and Λ^0 . At later times, two other peaks appear, one is caused by the μ^+ that comes from the decay of the K^+ and the other a μ^- from $\Lambda^0 \rightarrow p + \pi^-$ and $\pi^- \rightarrow \mu^- \bar{\nu}_\mu$.

Reaction 5 can be responsible for a potential background for proton decay in the LENA detector. For this case, only neutrinos with energies between 650 and 900 MeV can produce a signal with a signature similar to that of the proton decay. This neutrino energy window has been determined considering the energy window of proton decay events relevant for the analysis (150–650 MeV) and the energies deposited by the particles in the possible background events. The atmospheric neutrino flux has a maximum around 100 MeV and then decreases exponentially to higher energies. Assuming an energy dependence of $\phi_\nu \sim E_\nu^{-2.7}$ for the neutrino flux and a linear dependence for the cross-section, 10% of the total atmospheric neutrino flux occurs within the energy window considered in our analysis. Within this window a rate of 0.8 events per year (y^{-1}) caused by such neutrino reactions is predicted. To distinguish these background reactions from proton decay events the number of delayed electrons produced will be taken into account.

For proton decay in the channel considered, always one and only one electron is produced by the decay of the kaon. In the background reaction always two electrons are present, one from the μ^- decay and another from the K^+ decay chain. This fact considerably reduces the background contribution. Only in those cases where the energy of one of the background electrons is very small ($E < 0.5$ MeV) or when the signal of these electrons is hidden under that of the parent particle, the process exhibits only one electron. Events with electrons being hidden within the previous signal happen in 4% of the cases. From 200 muons simulated none of them had a decay electron with an energy smaller than 0.5 MeV. To estimate the number of background events of this type, the rate predicted has to be multiplied by this 0.04 and then, by two because electrons both from the μ^- and the K^+ decay chain can be hidden within the previous signal. Thus, the number of events of the type of reaction 5 expected in the LENA detector is 0.064 y^{-1} .

Other reactions where hadrons are produced are possible but all of them have lower rates and can also be distinguished from a proton decay signal by applying the arguments used for reactions 6 and 7.

C. Neutron Production by Cosmic Muons

Also very fast neutrons, generated by spallation processes of cosmic muons outside the detector, may reach the scintillator causing background. These neutrons are slowed down through scattering processes and the recoil protons may produce a background signal in the detector. However, only neutrons produced by muons passing close to the detector but not through the veto, have to be taken into account. In addition, these signals can be tagged as the neutrons are captured by hydrogen in the scintillator after $\sim 200 \mu\text{s}$, producing an observable 2.2 MeV γ -ray.

VI. PROTON DECAY SENSITIVITY

Once the time cut and the energy cut have been applied, one can calculate the final efficiency $\varepsilon = \varepsilon_E \cdot \varepsilon_T$ of the proton decay detection in the channel considered. In table I the efficiencies for events at different points of the detector are presented as well as the background rates for the same positions. As the detector is symmetrical along the cylinder axis the points considered are in the middle of the cylinder and at different radial distances. No dependence of the efficiency on the event position was found within the statistical error. This statistical error mainly comes from the time cut as the one from the energy cut is negligible. The background rates presented have been obtained by multiplying the muon background rate in the LENA detector (1190.4 y^{-1}) derived from the Super-Kamiokande experiment [9] with the background suppression from the time cut ($5 \cdot 10^{-5}$). The contribu-

TABLE I: For 1000 events produced at each radial position R in the detector, the efficiency in the time-cut ε_T , the efficiency in the energy-cut ε_E , the total efficiency ε including the statistical error, and the background rate B are given.

R (m)	ε_T	ε_E	ε (± 0.04)	B (y^{-1})
Center	0.649	0.995	0.65	0.11
3.0	0.675	0.994	0.67	0.11
6.0	0.650	0.994	0.65	0.11
9.0	0.679	0.995	0.68	0.11
11.5	0.666	0.995	0.66	0.11

TABLE II: Efficiencies ε for the detection of proton decay and photoelectron yield as function of attenuation, absorption and scattering lengths. The last column shows the time (see figure 2) at which the cut can be performed such that all background signals are rejected. Upper part: Different attenuation lengths for $\lambda_a = \lambda_s$. Bottom part: Attenuation length $\lambda = 10$ m for different combinations of λ_a and λ_s .

λ (m)	λ_a (m)	λ_s (m)	ε	Y (pe/MeV)	Cut (ns)
5	10	10	0.56	58	10
7	14	14	0.65	116	8
9	18	18	0.67	161	7
10	12	60	0.65	110	7
10	15	30	0.69	145	7
10	20	20	0.66	180	7
10	30	15	0.63	230	8
10	60	12	0.62	303	9

tion of the kaon production background (0.064 y^{-1}) has been added to the previous value.

In table II the efficiencies for proton decay detection and the photoelectron yield are given as function of different attenuation, absorption and scattering lengths. For the results presented, 1000 proton decay and 1000 background events were simulated for each combination of λ_a , λ_s and λ . All events were programmed to take place at the center of the detector. The last column of the table shows the time (see figure 2) at which the cut can be performed such that all background signals are rejected. In the upper part of the table, three attenuation lengths λ are presented keeping the contributions of absorption length and scattering length equal, $\lambda_a = \lambda_s$. As the attenuation length increases the photoelectron yield Y increases and the cut in the time intervals can be performed earlier. In the bottom part, the attenuation length has always the same value $\lambda = 10$ m and different values for the absorption and scattering lengths are given satisfying equation (1). The photoelectron yield increases as the absorption length increases because more optical photons reach the photomultipliers and therefore more photoelectrons are produced. As the scattering length increases, the cut in the time intervals can be performed earlier because the time information is better.

Table II shows that in all cases investigated, for $\lambda > 7$ m the efficiencies $\varepsilon > 0.62$. This is also true for

$\lambda_a = 12$ m and $\lambda_s = 60$ m, which we used for deriving the results presented earlier in figures 1 and 2. It demonstrates that the efficiency reachable is about tenfold enhanced compared to the efficiency reached in Super-Kamiokande for the same decay channel [9].

The activity for the proton decay is given by the expression:

$$A = \varepsilon N_p t_m / \tau \quad (8)$$

where $\varepsilon = 0.65$ is the efficiency already explained; $N_p = 1.45 \cdot 10^{34}$ is the number of protons in the detector; t_m is the measuring time and τ is the lifetime of the proton.

For the current proton lifetime limit for the channel considered ($\tau = 2.3 \cdot 10^{33}$ y) [10], about 40.7 proton decay events would be observed in LENA after a measuring time of ten years with about 1.1 background events. If no signal is seen in the detector within this ten years, the lower limit for the lifetime of the proton will be placed at $\tau > 4 \cdot 10^{34}$ y at 90% C.L. If one candidate is observed, the lower limit will be reduced to $\tau > 3 \cdot 10^{34}$ y at 90% C.L. and the probability of this event being background would be 32%.

VII. CONCLUSIONS

Within the simulations performed, an efficiency of $\sim 65\%$ for the search for proton decay in the LENA de-

tor has been determined. A lower limit for the proton lifetime of $\tau > 4 \cdot 10^{34}$ y (at 90% C.L.) can be reached if no proton decay event is measured within ten years.

The success in reaching this limit is based on the distinct pulse shape of the proton decay mode $p \rightarrow K^+ \bar{\nu}$ which is clearly observable in the LENA detector. Only a minor energy cut was used and hence the efficiency for observing the proton decay including free and bound protons is high. Since the values predicted by the favoured theories for the proton decay in this channel are of the order of the value resulting from our simulation, it is obvious that LENA measurements would have a deep impact on the proton decay research field. In order to further improve the results of the present simulation pulse shape analysis of higher precision will be performed.

Acknowledgments

We want to thank Prof. M. Lindner for the valuable discussions related to theory, D. D'Angelo, Dr. C. Lendvai and Dr. L. Niedermeier for detailed advice based on their experience from the BOREXINO experiment and Q. Weitzel for continuous help. This work has been supported by funds of the Maier-Leibnitz-Laboratorium (Garching) and by the Deutsche Forschungsgemeinschaft DFG (Sonderforschungsbereich 375).

-
- [1] L. Oberauer, F. von Feilitzsch, and W. Potzel, Nucl. Phys. B (Proc. Suppl.) **138**, 108 (2005).
 [2] S. Schoenert et al. (BOREXINO) (2004), submitted to Nucl. Instr. Meth. A, also physics/0408032.
 [3] C. Buck and M. Wurm, private communication (2005).
 [4] R. Svoboda (2003), Talk at the Eighth International Workshop on Topics in Astroparticle and Underground Physics (TAUP), Seattle, WA, USA, 5-9 September 2003.
 [5] H. Georgi and S. L. Glashow, Phys. Rev. Lett **32**, 438 (1974).
 [6] T. Hakaya, Nucl. Phys. B (Proc. Suppl.) **138**, 376 (2005).
 [7] S. Raby, *Proceedings of the 10th International Conference on Supersymmetry and Unification of Fundamental Interactions SUSY'02, DESY, Hamburg, Germany, 17-23 June 2002*, hep-ex/0211024.
 [8] K. S. Babu, J. C. Pati, and F. Wilczek, Phys. Lett. B **423**, 337 (1998).
 [9] Y. Hayato et al. (Super-Kamiokande), Phys. Rev. Lett **83**, 1529 (1999).
 [10] K. Kobayashi et al. (Super-Kamiokande), Phys. Rev. D **72**, 052007 (2005).
 [11] R. Arnowit, A. H. Chamseddine, and P. Nath, Phys. Lett. B **156**, 215 (1985).
 [12] K. Nakamura et al., Nucl. Phys. A **268**, 381 (1976).
 [13] T. Marrodán Undagoitia, *Search for the Proton Decay in the large liquid Scintillator Detector LENA*, Diploma Thesis, Technical University of Munich, May 2005.
 [14] S. Agostinelli et al. (Geant4), Nucl. Instr. Meth. A **506**, 250 (2003).
 [15] S. Eidelman et al. (Particle Data Group), Phys. Lett. B **592**, 1 (2004).
 [16] W. Leo, *Techniques for Nuclear and Particle Physics Experiments* (Springer-Verlag, Berlin, Heidelberg, 1987).
 [17] J. B. Birks, *The Theory and Practice of Scintillation Counting* (Pergamon Press, London, 1964).
 [18] H. O. Back et al. (BOREXINO), Phys. Lett. B **525**, 29 (2002).
 [19] G. Alimonti et al. (BOREXINO), Astropart. Phys **16**, 205 (2002).
 [20] D. Rein and L. M. Sehgal, Ann.of Phys. **133**, 79 (1981).
 [21] D. Rein, Z. Phys. C **35**, 43 (1987).
 [22] MINERvA Collaboration (2004), hep-ex/0405002.